JOURNAL OF APPLIED ELECTROCHEMISTRY 14 (1984) 537–545

Diphosphate coatings for protection of galvanized steel: quality control by impedance measurements

A. JARDY, R. ROSSET

Laboratoire de Chimie Analytique de l'Ecole Supérieure de Physique et de Chimie de Paris, 10 rue Vauquelin, 75231 Paris Cedex 05, France

R. WIART

Groupe de Recherche No. 4 du CNRS 'Physique des Liquides et Electrochimie' associé à l'Université Pierre et Marie Curie, 4 Place Jussieu, 75230 Paris Cedex 05, France

Received 21 December 1983

Galvanized steel surfaces can be protected against corrosion in natural waters by a superficial coating of zinc diphosphate, obtained by the partial oxidation of zinc in a solution containing diphosphate ions.

Impedance measurements were used to study the improvement in corrosion protection resulting from this layer and to develop a quality control method. The mechanism of both anodic and cathodic processes remains the same in the presence of the coating as in its absence, so that the relationship

$$R_t I_{corr} = \text{constant}$$

is valid (R_t is charge transfer resistance; I_{corr} is intensity of the corrosion current). Thereby, a protection factor, defined as the ratio of the corrosion currents in the absence and in the presence of the coating, can be estimated from the corresponding charge transfer resistances determined experimentally from impedance diagrams.

Impedance data obtained on several test-pieces are in good agreement with the coating morphology, as shown by direct scanning electron microscope (SEM) observations, leading to a simple criterion for quality control.

1. Introduction

Galvanized steel surfaces can be protected against corrosion in natural waters by a superficial coating of zinc diphosphate (pyrophosphate), obtained by the partial oxidation of galvanization zinc [1–3]. In the process which is the object of this study, this oxidation is realized chemically by dissolved oxygen acting as the oxidant, and is catalysed by the nitrate–nitrite system, in a solution containing diphosphate ions at a pH corresponding to the $Zn_2P_2O_7$ solubility minimum [4, 5]. Fig. 1 shows that there is a sharp optimum pH value, depending on the diphosphate ion concentration. The ability to heal possible defects on the coating electrochemically by anodic polarization of testpieces in this solution at the end of the chemical treatment was also studied [6]. Coating formation (at the pH considered) occurs according to:

$$2Zn\downarrow + 3H_2P_2O_7^{2-} - 4e^- \rightarrow Zn_2P_2O_7\downarrow + 2H_3P_2O_7^- \quad (1)$$

The aim of this paper is to describe a method based on impedance measurements for the quality control of the coating and the estimation of the resulting improvement in corrosion protection. Direct measurement of the corrosion rate by determining weight loss during immersion in a corrosive medium would be an absolute method, but it is unwieldy and too time-consuming for systematic control. It has been shown by Epelboin and co-workers [7, 8] that a.c. impedance measurements give more accurate and reliable results in the corrosion-rate determination than methods based on polarization resistance measurements.

0021–891X/84 $03.00 + .12

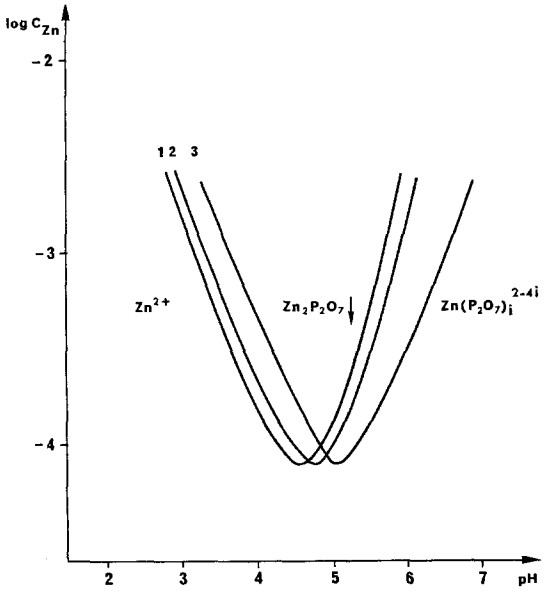

Fig. 1. The pH dependence of zinc diphosphate total solubility in diphosphate solutions of various concentrations. Curve 1 - 10^{-1} M; Curve 2 - 5×10^{-2} M; Curve 3 - 10^{-2} M.

2. Experimental details

Electrolytes were prepared using Merck analytical grade chemicals and water doubly distilled in quartz. The electrolytes were deoxygenated with argon before and during measurements and were maintained at constant temperature at 26° C. The auxiliary electrode was a platinum gauze cylinder of large area and potentials were measured against a saturated K_2SO_4 mercurous sulphate electrode (SSE, $E_{ref} = 0.40$ V vs SCE). The working electrode was either a rotating disc electrode or a static electrode. In the first case, it was a cut from a high purity zinc cylinder (Johnson Matthey, 99.999%) of 0.2 cm^2 area, the lateral wall of which was insulated with 'Specifix' resin. In the second case, the discs used were 2 cm in diameter and 2 mm thick (area 7.3 cm^2); the electrical contact was made with a copper wire insulated with an epoxy resin. These discs were made from either hot-dip galvanized steel or from industrial zinc (zinc used for galvanization). A typical chemical analysis of industrial zinc is given in Table 1.

In the case of bare zinc, electrodes were prepared by polishing with emery paper (Grade 600) followed by immersion for a few seconds in approximately 2 M HCl solution and water rinsing.

I–E current–potential curves were obtained galvanostatically except for current plateaux which were recorded potentiostatically. The potential, E, measured vs the SSE reference electrode was corrected for the ohmic drop obtained from the high-frequency limit of the impedance.

The complex electrode impedance, $Z = R - jG$, was measured using a digital transfer function analyser (Solartron Schlumberger 1174), coupled to a home-made regulation device. Complex plane impedance plots were automatically set out on an X–Y recorder (Sefram TGM 164).

After the impedance measurements, some electrodes were observed in a scanning electron microscope (SEM) and photographs were taken.

3. Results and discussion

3.1. *Electrolyte choice*

Electrochemical techniques (current–potential curves and a.c. impedance measurements) require the presence of a supporting electrolyte in order to render the solution sufficiently conductive. This is the reason why the determination of the corrosion protection effect cannot be regarded as an

Table 1. Impurity content of industrial zinc (99.5% RCA Special)

lead	cadmium	tin	iron	copper	aluminium
0.35%	0.0048%	0.0003%	0.012%	0.0015%	0.0012%

absolute one* but as a relative one, obtained by comparing the behaviour, in the selected electrolyte, of galvanized steel with or without a protective coating. Therefore, the electrolyte was chosen to give highly reproducible results, and preferably a simple mechanism for both anodic and cathodic reactions. Thus the electrolyte chosen was the following: 0.5 M sodium sulphate buffered at pH 4.7 with 10^{-2} M acetate buffer and deaerated by argon bubbling. The current–potential curves obtained with a rotating disc electrode made of high purity zinc, and impedance plots obtained at typical points on the curve are shown in Fig. 2. It has been found experimentally that the presence of the buffer and the deoxygenation of the solution were necessary conditions to give reproducible results. Without a buffer, pH varied and impedance plots in the anodic region became time-dependent.

In the selected electrolyte, the plateau observed in reduction is under diffusion control and corresponds to the reduction of the acetic acid in the buffer. This diffusion limitation is also apparent on the impedance diagram, which is typical of a diffusion impedance coupled with the charge transfer resistance and the double-layer capacitance. The impedance plot corresponding to zinc dissolution mainly involves a charge transfer (charge transfer resistance and double-layer capacitance in parallel) but also reveals an inductive loop with the beginning of an additional capacitive loop at low frequencies. This diagram is similar to those obtained in chloride medium [9, 10]; however, the low-frequency portion of the diagram is much smaller, and the characteristic frequency of the inductive loop is lower. This low-frequency part most likely corresponds to a multi-step mechanism for zinc dissolution involving the formation of adsorbed intermediates and possibly insoluble products such as oxide or hydroxide. In a sulphate medium, the polarization resistance appears nearer the charge transfer resistance and the electrode kinetics are different from those in a chloride medium where Cl^- stimulates the dissolution. At

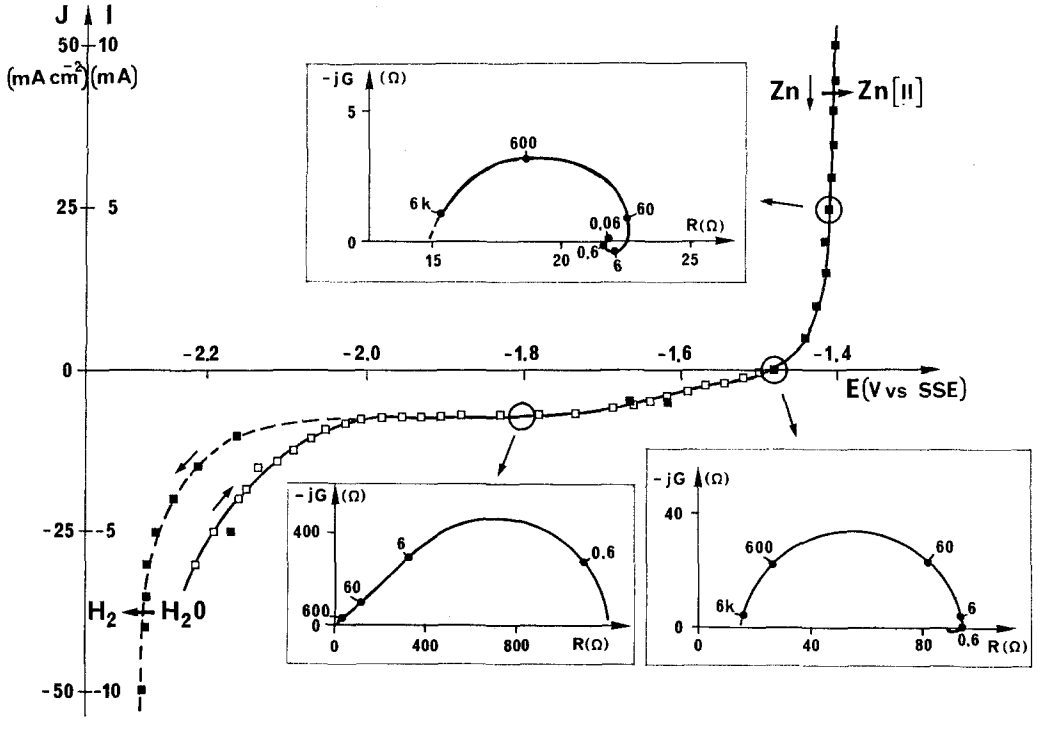

Fig. 2. Current–potential curves and complex plane impedance plots (frequency in Hz) at indicated points, obtained with a rotating-disc electrode (Ω = 1500 r.p.m.) in deoxygenated 0.5 M Na_2SO_4 + 10^{-2} M acetate buffer. ■ – under galvanostatic control; □ – under potentiostatic control.

* It would be necessary to determine corrosion current density in a wide range of natural waters where the results would be dependent on composition.

the equilibrium potential, regulated galvanostatically by imposing $I = 0$, the impedance diagram shows only a semicircular loop corresponding to charge transfer. The dimensions of this loop are roughly independent of the electrode rotation speed, which means that mass transfer is not a significant factor for the cathodic reaction near the corrosion potential. At this potential the cathodic (reduction of oxidant present in the electrolyte) and the anodic (dissolution of metal) reactions occur on different parts of the electrode surface, the current balance equation being:

$$I_a = -I_c = I_{corr} \qquad (2)$$

where I_a is anodic current, I_c is cathodic current and I_{corr} is corrosion current (all microcells being shortcircuited at the free corrosion potential so that $I = 0$).

From the above results, it can be concluded that, at the corrosion potential, both anodic and cathodic interfacial reactions are under charge transfer control. If it is shown experimentally that the mechanism of both reactions is not modified by the presence of the $Zn_2P_2O_7$ coating according to the equation:

$$R_t I_{corr} = \text{constant} \qquad (3)$$

R_t being the charge transfer resistance, then the ratio of the charge transfer resistances will give the ratio of corrosion currents and therefore allow an estimation of the corrosion protection resulting from the presence of the protective layer.

Moreover, the absence of mass transfer control allows the use of static electrodes, such as large area test-pieces of galvanized steel. This decreases the charge transfer resistance, which is inversely proportional to the electrode surface area, and therefore impedance measurements on pre-passivated electrodes are made easier.

3.2. *Charge transfer reactions*

Experimental results were poorly reproducible when plotting current–potential curves or impedance diagrams for rough galvanized steel electrodes, and were not convenient for the estimation of standard conditions for protection. Therefore, electrodes made of pure zinc (used for industrial galvanizing) were used for this purpose. Such test-pieces could be chemically cleaned (for example with HCl) and mechanically polished, operations which were impossible in the case of galvanized steel plate. Therefore the surface state was well-defined and reproducible.

Current–potential curves obtained respectively with polished pure zinc, rough galvanized steel and chemically coated galvanized steel are shown in Fig. 3. These curves show that both cathodic and anodic reactions are strongly inhibited, particularly the latter (see below), in the presence of the zinc diphosphate coating. This is a good indication that protection against corrosion is enhanced. In addition, it appears that rough galvanized steel is slightly more difficult to oxidize than pure zinc. This is probably due to a natural passivation, for example, by the formation of a partial oxide layer during air-cooling after hot-dip galvanization. This passivation appears also, but with bad repro-

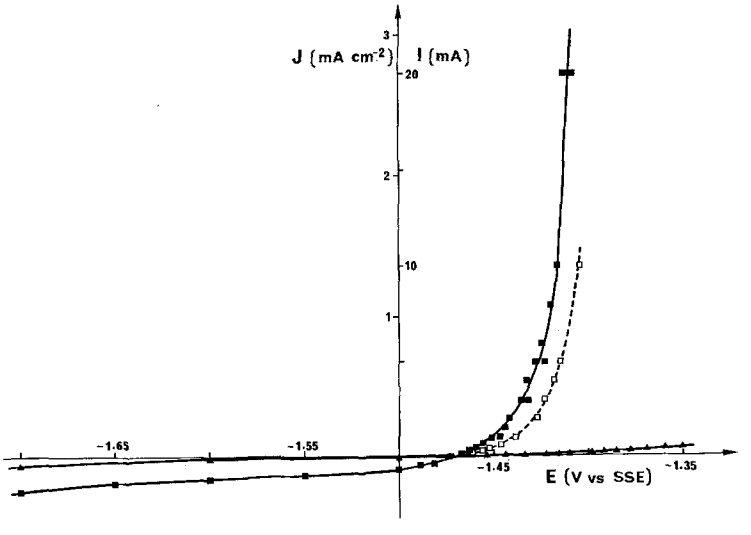

Fig. 3. Current–potential curves obtained with static electrodes ($A = 7.3\ cm^2$) ■ – industrially pure zinc; □ – rough galvanized steel; ▲ – $Zn_2P_2O_7$-coated galvanized steel. Same electrolyte as in Fig. 2.

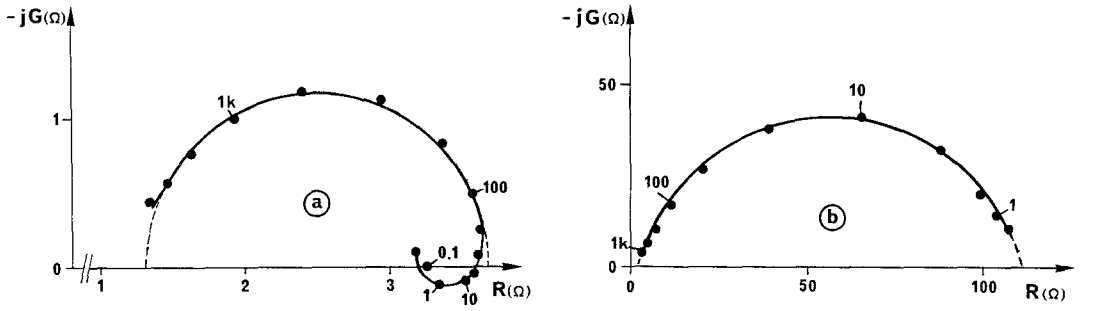

Fig. 4. Complex plane impedance plots (frequency in Hz) obtained during zinc dissolution ($E \approx -1400$ mV vs SSE) with: (a) industrially pure zinc ($I_{dc} = 10$ mA); (b) $Zn_2P_2O_7$-coated galvanized steel ($I_{dc} = 0.20$ mA). Same electrolyte as in Fig. 2.

ducibility, on the impedance plots at the corrosion potential and the transfer resistance is greater (sometimes up to 50%) than that observed on pure zinc.

In order to study the influence of the protective layer on the mechanism of both the anodic reaction (zinc dissolution) and cathodic reaction (reduction of acetic acid), impedance diagrams were plotted at different potentials, either on industrially pure zinc or $Zn_2P_2O_7$ coated galvanized steel electrodes. Typical impedance diagrams obtained in oxidation, at a potential close to -1400 mV vs SSE, are shown in Fig. 4. The transfer resistance, R_t, is easily deduced from the capacitive loop plotted at high frequencies. The presence of the coating produces an increase in R_t and a decrease in the d.c. intensity, I, so that the product R_tI remains constant, i.e. equal to 24 mV. This R_t increase indicates a strong inhibition of zinc dissolution due to the coating. Simultaneously, the mean value of the double-layer capacity (calculated from the characteristic frequency and disregarding the dispersion observed for the coated electrode) remains about the same: respectively, 18 and 13 μF cm^{-2}. The experimental R_t determination therefore requires a frequency sweep down to lower values in the presence of the coating than in its absence. In addition, impedance plots obtained during the dissolution of industrially pure zinc reveal at least one inductive loop at low frequencies, the characteristic frequency of which is near 1 Hz. This indicates the existence of a multistep mechanism involving adsorbed species, as for high-purity zinc.

Typical impedance diagrams, obtained by cathodic polarization at potentials close to -1700 mV vs SSE, are shown in Fig. 5. A diffusion-limiting effect is indicated only at low frequencies because of the absence of agitation, i.e. in natural convection conditions. In both cases, charge transfer resistances can be determined accurately by extrapolation leading to similar values of the product R_tI; respectively, 60 and 88 mV. However, it is noticeable that the cathodic process is slowed down to a far lesser extent than the anodic one, in the presence of the protective

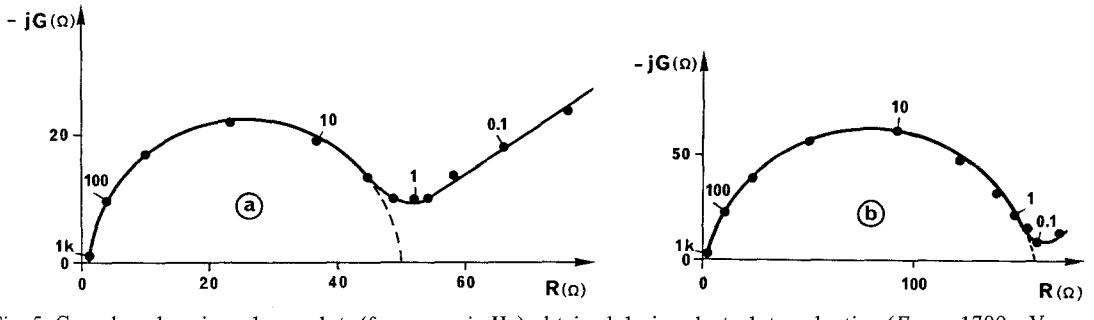

Fig. 5. Complex plane impedance plots (frequency in Hz) obtained during electrolyte reduction ($E = -1700$ mV vs SSE) with: (a) industrially pure zinc ($I_{dc} = -1.38$ mA); (b) $Zn_2P_2O_7$-coated galvanized steel ($I_{dc} = -0.50$ mA). Same electrolyte as in Fig. 2.

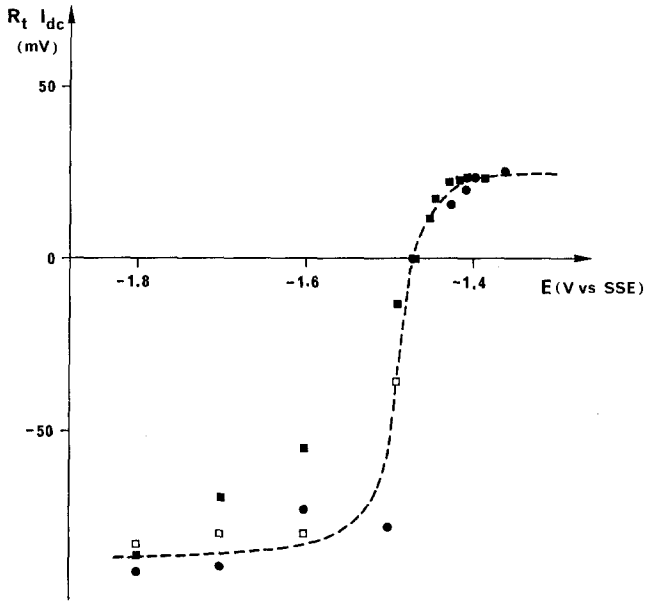

Fig. 6. Potential dependence of the product (transfer resistance R_t × current I): ■ – industrially pure zinc, unstirred solution; □ – industrially pure zinc, stirred solution; ● – $Zn_2P_2O_7$-coated galvanized steel, unstirred solution.

layer. These results, in good agreement with the I–E curves shown in Fig. 3, are consistent with the following interpretations:

(a) the coating is not very conducting (this is also demonstrated by the increase in the ohmic drop), and offers a residual conductivity

(b) the coating produces a specific inhibition of the anodic process.

The value of the double-layer capacity again decreases slightly in the presence of the coating at 24 and 12 μF cm^{-2}, respectively.

The potential dependence of the product R_tI is depicted in Fig. 6. It appears that this product reaches the same limiting values in the anodic and the cathodic ranges, for pure zinc and for chemically coated galvanized steel electrodes. In addition, the cathodic limiting effect appears independent of the solution agitation. These observations demonstrate that both anodic and cathodic processes obey Tafel laws according to:

$$I_a = I_a^0 \exp(b_a E) \quad (4)$$

and

$$I_c = I_c^0 \exp(-b_c E) \quad (5)$$

(b_a and b_c being the Tafel coefficients) and that the presence of the $Zn_2P_2O_7$ layer does not change b_a and b_c values, but decreases I_c^0 and, mainly, I_a^0, i.e. the rate constant of zinc dissolution.

Tafel coefficients, b_a and b_c, are deduced from the limiting values of the product R_tI as follows

For b_a, from the maximum value reached in the anodic oxidation range ($E \gg E_{eq}$) R_tI_a = 24 mV. By differentiating Equation 4, we obtain:

$$\frac{1}{R_t} = \frac{dI_a}{dE} = b_aI_a \quad (6)$$

thus:

$$b_a = \frac{1}{R_tI_a} = 42V^{-1} \quad (7)$$

For b_c, from the minimum value reached in the cathodic reduction range ($E \ll E_{eq}$) $R_tI_c \approx$ − 85 mV. By differentiating Equation 5, we obtain:

$$\frac{1}{R_t} = \frac{dI_c}{dE} = -b_cI_c \quad (8)$$

thus:

$$b_c = -\frac{1}{R_tI_c} = 12V^{-1} \quad (9)$$

The activation of both anodic and cathodic processes with potential remain the same with or without the protective layer. The product of the charge transfer resistance and the corrosion current intensity, I_{corr}, at the free corrosion potential is given by:

$$R_tI_{corr} = \frac{1}{b_a + b_c} \quad (10)$$

and is constant thus allowing I_{corr} to be estimated.

3.3. *Protection determination and quality control*

We define the protection factor, f, resulting from the coating as: the ratio of corrosion intensities in the selected electrolyte of test-pieces of identical dimensions, the first in industrially pure zinc (I_{corr}) and the second in $Zn_2P_2O_7$ coated galvanized steel (I'_{corr}). According to Equation 10, f is given by the inverse ratio of charge transfer resistances measured at the free corrosion potential; so we have:

$$f = \frac{I_{corr}}{I'_{corr}} = \frac{R'_t}{R_t} \qquad (11)$$

Typical examples of impedance diagrams obtained at the equilibrium potential ($I = 0$, under galvanostatic control) with the two types of electrodes are given in Fig. 7. In both cases, the capacitive loops corresponding to the charge transfer are well defined and the transfer resistances easily deduced from the diameter of the loop, as indicated on the graphs. From the experimental results, $R_t = 32\,\Omega$ and $R'_t = 1070\,\Omega$, the value $f = 33.5$ is calculated. The corrosion inhibition is quite good as the corrosion-rate is divided by this factor in the presence of the coating.

Transfer resistance measurements at the free corrosion potential have been applied to several industrially pure zinc test-pieces and the statistical analysis of the results gives:

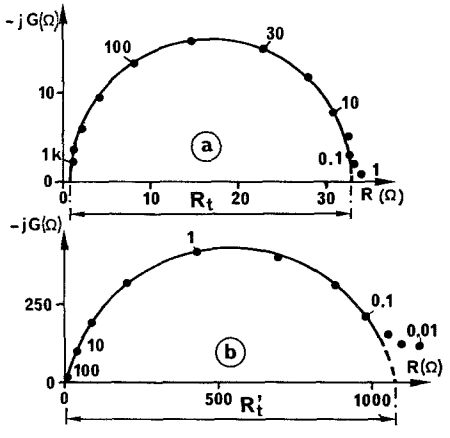

Fig. 7. Complex plane impedance plots (frequency in Hz) obtained at free corrosion potential, E_{corr} in deoxygenated 0.5 M Na_2SO_4 + 10^{-2} M acetate buffer with: (a) industrially pure zinc; $E_{corr} = -1470$ mV vs SSE, (b) $Zn_2P_2O_7$-coated galvanized steel; $E_{corr} = -1439$ mV vs SSE.

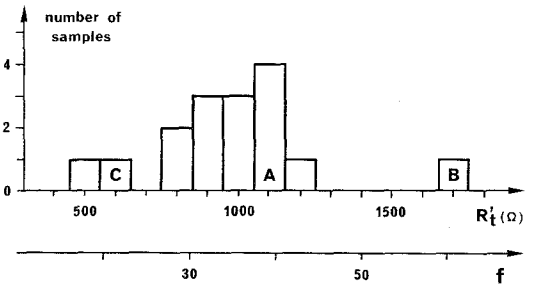

Fig. 8. Histogram of transfer resistances, R'_t and protection factor, f, for $Zn_2P_2O_7$-coated galvanized steel test-pieces.

$$R_t = (28 \pm 7.5)\Omega \qquad (12)$$

at a 0.9 confidence level.

The dispersion may indicate some inhomogeneity in the impurity content of the zinc bar used for the preparation of the electrodes.

The method above has been applied to sixteen different test-pieces of $Zn_2P_2O_7$ coated galvanized steel, each determination being at least duplicated. The results are shown as a histogram in Fig. 8. Calculated f values are reported on a scale below.

It is noticeable that the coating morphology is correlated to the impedance data, as depicted on Fig. 9. On the one hand, Electrode B, which has the largest resistance transfer, reveals a more homogeneous layer than Electrode A. The former received electrochemical post-treatment (anodic polarization at E_{eq} + 100 mV for 30 min at the end of the chemical treatment in solution) while the latter had been chemically coated only. On the other hand, test-pieces for which the transfer resistance is found to be lower than 700 Ω, do not offer sufficient protection. Contrary to the previous electrodes (which give reproducible or even increasing R'_t values) such electrodes give R'_t values decreasing with time from one plot to the other. This is a sign of the gradual degradation of the coating. As seen in Fig. 9c, large gaps are apparent in the protective layer. Energy-dispersive X-ray analysis shows that these are not due to a lack of zinc but to a layer inhomogeneity. A possible explanation is that mechanical degradation of the coating due to hydrogen evolution takes place on some parts of the surface acting as microcathodes in the corrosion process. These observations lead us to conclude that for quality control the minimum R'_t value required for good protection is 700 Ω corresponding to $f = 25$. Furthermore,

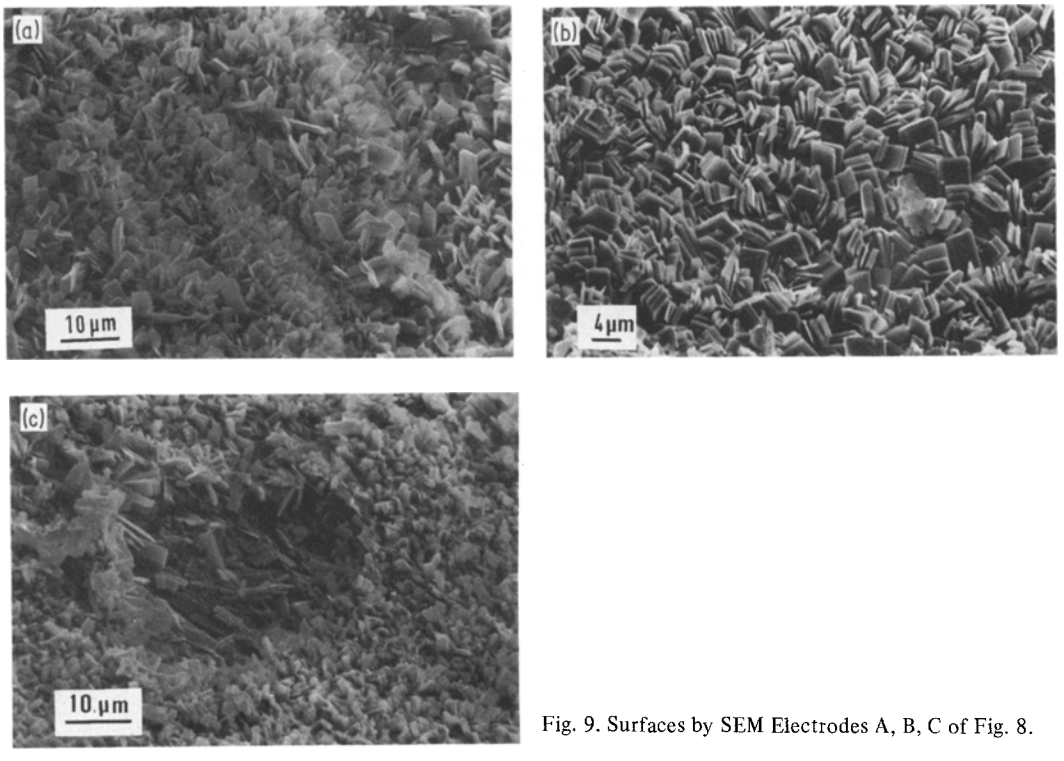

Fig. 9. Surfaces by SEM Electrodes A, B, C of Fig. 8.

the increase in R'_t observed in the case of well-protected surfaces is consistent with a consolidation of the coating which may have two origins:

(a) the conversion of zinc diphosphate to a more stoichiometric form because of the oxidation of zinc into Zn^{2+} ions, or the formation of more $Zn_2P_2O_7$ which involves adsorbed diphosphate ions

(b) the healing of defects in the coating resulting from the precipitation of oxide or hydroxide.

However, direct SEM observation does not show different types of crystals in the layer and the first hypothesis seems more likely. In any case, the presence of a slow passivating reaction in the mechanism of layer formation is consistent with the second capacitive loop observed at low frequencies for coated electrodes (Fig. 10): when the diameter of the second loop decreases, the diameter of the first one increases and the protection becomes better.

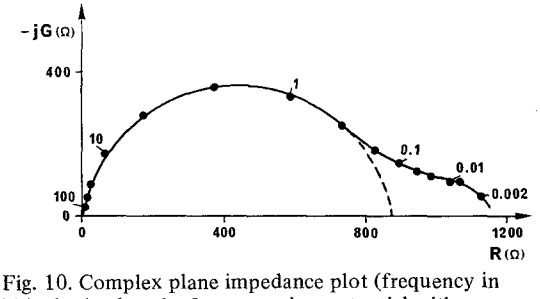

Fig. 10. Complex plane impedance plot (frequency in Hz) obtained at the free corrosion potential with a coated electrode, down to low frequencies. Same electrolyte as in Fig. 2.

With pure zinc electrodes, the inductive loop, at low frequencies and at the corrosion potential, is always smaller than on diagrams plotted in the oxidation domain, so that R_p, the polarization resistance, is only slightly lower than R_t.

In addition, it is noticeable that, as previously, the double layer capacity determined at the free corrosion potential is scarcely affected by the presence of the coating. As shown earlier, R'_t is largely greater than R_t and therefore, the determination of the former needs much lower frequency values than in the absence of zinc diphosphate. As seen in Fig. 7, whereas R_t could be easily measured with a frequency sweep down to 1 Hz, R'_t could not be correctly determined under the same conditions. This is why the use of classical methods for the determination of polarization resistance would possibly give wrong results.

The apparent constancy of the double layer capacity and the reduction in the active electrode area due to the layer may be considered as compatible in view of the morphology of the coating. From the micrographs, it appears that the true electrochemical surface area is much larger than the geometric area of the electrodes. In addition, the porous structure of the layer and its slight conductivity are also consistent with the flattening of the capacitive loop [11], which is a semi-circle for the pure electrode.

For the corrosion of pure zinc electrodes, the existence of a multi-step mechanism involving adsorbed species and insoluble products was confirmed in an attempt to measure the corrosion rate directly: the amount of zinc appearing in the electrolyte is lower than that predicted from the value of I_{corr} (assumed constant) and the rate of dissolution becomes slower with time. Due to the partition of the oxidation products between insoluble species remaining on the surface and soluble Zn^{2+} ions, the corrosion rate cannot be determined accurately by weight-loss experiments or chemical analysis, whereas it is easily obtained from impedance measurements.

4. Conclusion

A.c. impedance measurements are well suited for the determination of the corrosion protection effect of zinc diphosphate coatings on galvanized steel. The protection factor can be deduced easily from the ratio of the transfer resistances at the free corrosion potential in the presence or absence of the coating. With electrochemical post-treatment of the chemically-coated surfaces, the corrosion rate is reduced by a factor as high as 50.

Moreover, systematic study has shown that the protection of galvanized steel against corrosion is guaranteed for a long time only when the transfer resistance is higher than a minimum value, which corresponds to a protection factor of 25. This criterion, accurate and easy-to-use, is a measurement of the protective layer quality.

Acknowledgement

This work was supported by the International Lead and Zinc Research Organization and by Chaffoteaux et Maury. One of the authors (A.J.) expresses his appreciation to Dr. Froment, Head of the Groupe de Recherche No. 4 du Centre National de la Recherche Scientifique 'Physique des Liquides et Electrochimie' who allowed him the opportunity to join the laboratory for one year.

References

[1] N. Dreulle and M. Longuepee, French Patent No. 7 402 178 (1974).
[2] P. Dreulle, M. Longuepee and D. Dhaussy, French Patent No. 7 637 425 (1976).
[3] M. Longuepee, D. Dhaussy, P. Dreulle N. T. Dung and J. C. Bavay, *Rev. Met.* **75** (1978) 385.
[4] R. Rosset, A. Jardy and N. Parthasarathi, 'Protection of galvanized steel against cold and hot water corrosion by a pyrophosphate coating', Paper 12, Intergalva, London (1982).
[5] R. Rosset and A. Jardy, French Patent No. 8 022 605 (1980).
[6] *Idem*, French Patent No. 7 814 950 (1978) and US Patent No. 4 243 496 (1981).
[7] I. Epelboin, M. Keddam and H. Takenouti, *J. Appl. Electrochem.* **2** (1972) 71.
[8] I. Epelboin, C. Gabrielli, M. Keddam and H. Takenouti, 'Electrochemical Corrosion Testing', ASTM Special Technical Publication 727 (1981) pp. 150–66.
[9] C. Cachet and R. Wiart, *J. Electroanal. Chem.* **111** (1980) 235.
[10] *Idem, ibid.* **129** (1981) 103.
[11] R. de Levie, 'Advances in Electrochemistry and Electrochemical Engineering', Vol. 6, Interscience-Wiley, New York (1967) pp. 329–97.